

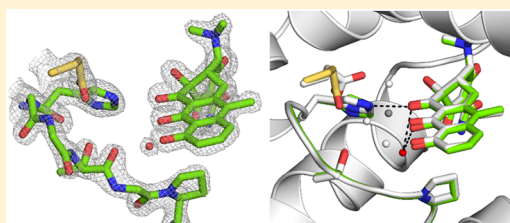
Tetracycline Repressor Allostery Does Not Depend on Divalent Metal Recognition

Sebastiaan Werten,* Daniela Dalm, Gottfried Julius Palm, Christopher Cornelius Grimm, and Winfried Hinrichs*

Department of Molecular Structural Biology, Institute for Biochemistry, University of Greifswald, Felix-Hausdorff-Strasse 4, D-17487 Greifswald, Germany

S Supporting Information

ABSTRACT: Genes that render bacteria resistant to tetracycline-derived antibiotics are tightly regulated by repressors of the TetR family. In their physiologically relevant, magnesium-complexed form, tetracyclines induce allosteric rearrangements in the TetR homodimer, leading to its release from the promoter and derepression of transcription. According to earlier crystallographic work, recognition of the tetracycline-associated magnesium ion by TetR is crucial and triggers the allosteric cascade. Nevertheless, the derivative 5a,6-anhydrotetracycline, which shows an increased affinity for TetR, causes promoter release even in the absence of magnesium. To resolve this paradox, it has been proposed that metal-free 5a,6-anhydrotetracycline acts via an exceptional, conformationally different induction mode that circumvents the normal magnesium requirement. We have tested this hypothesis by determining crystal structures of TetR–5a,6-anhydrotetracycline complexes in the presence of magnesium, ethylenediaminetetraacetic acid, or high concentrations of potassium. Analysis of these three structures reveals that, irrespective of the metal, the effects of 5a,6-anhydrotetracycline binding are indistinguishable from those of canonical induction by other tetracyclines. Together with a close scrutiny of the earlier evidence of a metal-triggered mechanism, these results demonstrate that magnesium recognition per se is not a prerequisite for tetracycline repressor allostery.



Bacterial resistance to tetracycline [Tc (Figure 1)] and its derivatives is regulated by the tetracycline repressor (TetR) family of transcription factors.^{1,2} In the absence of antibiotic, TetR homodimers interact with palindromic elements in the promoter of the resistance gene, thereby blocking its transcription. This resistance gene encodes an efflux pump, such as TetA, whose untimely expression would be detrimental to bacterial fitness. When Tc binds to TetR, the repressor dimer undergoes an allosteric transition that affects the distance between the two DNA-binding domains as well as their relative orientation^{3–6} and rigidity.⁷ As the resulting arrangement is incompatible with the fixed spacing between the symmetry-related half-sites in the operator DNA, the repressor dissociates from the promoter, allowing initiation of transcription.

Because of its prominent role in antibiotic resistance as well as its practical use in genetically engineered regulatory networks, TetR has been intensively studied for several decades. Moreover, the repressor is an important model system for allosteric gene regulation at the transcription level.¹ Despite the extensive body of experimental data currently available, questions remain about the precise mechanism responsible for transmission of the allosteric effect to the distal DNA-binding domains, which are located >20 Å from the Tc-binding pockets. In particular, the exact role of the Tc-associated Mg²⁺ ion continues to be controversial.^{8,9}

In vivo, Tc strongly interacts with divalent metal ions, which it chelates via its ketoenolate moiety (Figure 1). Although various metals can be bound in this manner, earlier work has shown that the complex with Mg²⁺ is the prevalent form of the antibiotic under physiological conditions.¹⁰ In crystal structures of liganded TetR, the Mg²⁺ ion and several water molecules in its coordination sphere interact with protein side chains thought to play a role in early structural changes, such as His100 and Thr103.¹ This has led to the hypothesis that the precise positioning of the Mg²⁺ ion is the actual cue that triggers the allosteric effects, via sequestration of the aforementioned side chains.⁵ Direct support for this idea has come from a crystallographic study of partially and completely Mg²⁺-depleted complexes of a class D TetR [TetR(D)] bound to 7-chlorotetracycline [CTc (Figure 1)], as reported by Orth et al.⁸ The complexes in question were prepared via cocrystallization of the repressor with CTc and a 1:4 mixture (molar ratio) of Mg²⁺ and EDTA or by washing existing crystals of the Mg²⁺-containing complex with highly concentrated EDTA. The former procedure resulted in a crystal structure in which one binding site of the TetR dimer contains Mg²⁺-complexed CTc and the other the Mg²⁺-free antibiotic. For the EDTA-washed form, a symmetrical dimer was reported in

Received: October 12, 2014

Revised: November 27, 2014

Published: November 28, 2014



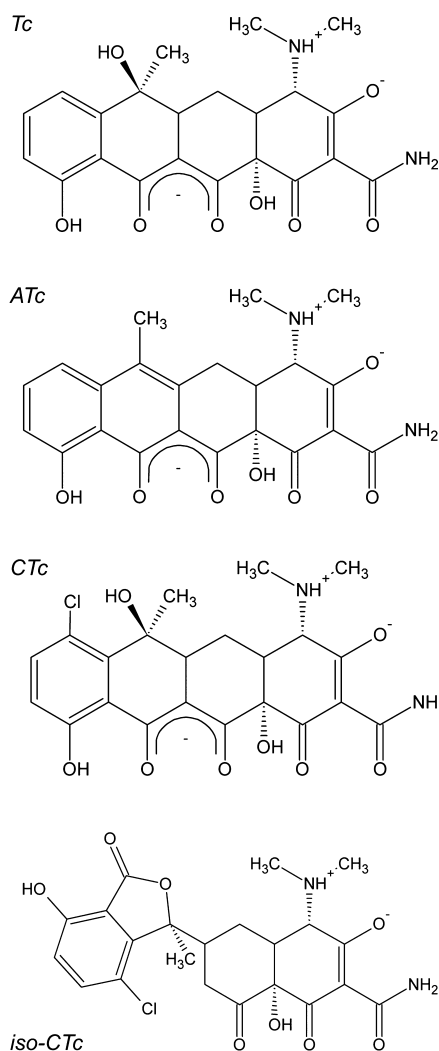


Figure 1. Structures of tetracycline (Tc, also termed 7H-Tc), 5a,6-anhydrotetracycline (ATc), 7-chlorotetracycline (CTc), and 6-iso-7-chlorotetracycline (iso-CTc). For the first three structures, ionized forms whose ketoenolate moieties (depicted with a delocalized negative charge) chelate Mg^{2+} under physiological conditions are shown.

which both repressor subunits contain Mg^{2+} -free CTc. Invariably, depletion of Mg^{2+} from a binding site caused the corresponding subunit to remain in the uninduced state, despite the presence of CTc. The authors therefore concluded that the metal ion acts as a trigger for the allosteric transition.⁸

According to detailed models that recapitulate the available data,^{1,5,8,11} TetR induction occurs in a stepwise manner and involves a series of hypothetical intermediates. The first of these is binding of the antibiotic via its hydrophobic face and several hydrogen bonds to a rigid part of the binding pocket, an event that does not provoke any structural changes in the protein. This is followed by sequestration of the side chains of His100 and Thr103 by the now precisely positioned Mg^{2+} ion, which requires unwinding of the C-terminal extremity of helix $\alpha 6$ (residues 100–102). As a result, residues 100–103 form a type II β -turn, a structural feature generally considered the hallmark of TetR induction.¹ In subsequent stages, rotation of helix $\alpha 4$ and a pendulum-like motion of the DNA-binding domain are thought to follow. Indeed, these downstream events were observed in molecular dynamics simulations when early

structural changes in the immediate vicinity of $[MgTc]^+$ were imposed by means of harmonic restraints.¹¹

Although metal-dependent models for repressor allostery elegantly explain most of the experimental data, certain observations remain enigmatic and seem to argue against a central role for Mg^{2+} . In particular, the high-affinity ligand 5a,6-anhydrotetracycline [ATc (Figure 1)] was found to release TetR from promoter DNA in the presence and absence of divalent metal ions.⁹ This observation led Scholz et al.⁹ to postulate the existence of an alternative as yet uncharacterized induction mode, potentially unique to ATc, which bypasses the metal requirement. In the study presented here, we have directly investigated the role of Mg^{2+} in TetR induction by ATc via crystallographic analysis of the TetR(D)– $[MgATc]^+$ complex. In addition, we analyzed the corresponding Mg^{2+} -free complex, which we prepared in the presence of EDTA. We also investigated the question of whether a monovalent ion such as K^+ can substitute for Mg^{2+} . Earlier work involving the TetR(D)– $[MgTc]^+$ complex had already established that Mg^{2+} can be replaced by various other divalent metal ions (including Mn^{2+} , Ca^{2+} , Ni^{2+} , and Co^{2+}) without affecting the structure of the induced complex.¹⁰ In contrast, binding of monovalent ions to TetR–inducer complexes had not been investigated before. For this reason, we also crystallized the Mg^{2+} -free TetR(D)–ATc complex in the presence of high concentrations of KCl.

EXPERIMENTAL PROCEDURES

TetR(D) was expressed and purified as described previously.^{12,13} Prior to crystallization, the protein was concentrated to 10–20 mg/mL using spin dialysis tubes (Vivaspin 15, 10 kDa molecular mass cutoff, Sartorius Stedim Biotech). All TetR(D)–ATc complexes were crystallized using the hanging drop method at 22 °C, essentially as described previously.⁴ Crystals were cryoprotected by means of paraffin oil and subsequently flash-frozen in liquid nitrogen.

X-ray diffraction data were collected at 100 K on beamlines X12 (in the case of the Mg^{2+} -free complex prepared in the presence of EDTA) and X13 (the complexes with Mg^{2+} and K^+) of the EMBL outstation at DESY (Hamburg, Germany). Data from these beamlines were processed using HKL-2000¹⁴ and XDS,¹⁵ respectively. All subsequent crystallographic calculations were conducted using the CCP4 package.¹⁶ Specifically, the structures were determined by means of molecular replacement (MR) using AMoRe¹⁷ and the structure of the TetR(D)– $[MgTc]^+$ complex [Protein Data Bank (PDB) entry 2TRT], from which the ligand had been removed, as the search model. This was followed by multiple rounds of manual model building and refinement using Coot^{18,19} and Refmac.^{20,21} An overview of data collection and structure refinement statistics can be found in Table 1. Figures showing molecular models were prepared using CCP4MG²² and PyMOL (0.99rc6, DeLano Scientific). Structures and X-ray diffraction data for the Mg^{2+} -containing complex, the K^+ -containing complex, and the metal-free complex in the presence of EDTA have been deposited in the PDB as entries 4D7M, 4D7N, and 2XPU, respectively.

TetR(D)–ATc association constants in the presence and absence of K^+ were determined at 20 °C as described by Palm et al.¹⁰ in a buffer containing 50 mM Tris (pH 8.0), 0.1 mM EDTA, and 150 mM NaCl or KCl. A TetR(D) concentration of 0.1–1 μ M was used in these experiments.

For analysis of the earlier structures 1BJY and 1BJO determined by Orth et al.,⁸ the original diffraction data

Table 1. Data Collection and Refinement Statistics for the Determination of the Structure of the Three TetR(D) Complexes with ATc^a

	TetR(D) with ATc and Mg ²⁺ (PDB entry 4D7M)	TetR(D) with ATc and K ⁺ (PDB entry 4D7N)	TetR(D) with ATc (PDB entry 2XPU)
Data Collection			
source	X13	X13	X12
wavelength (Å)	0.80	0.80	1.0
detector	MAR CCD (SX-165)	MAR CCD (SX-165)	MAR CCD (MX-225)
space group	<i>I</i> ₄ 22	<i>I</i> ₄ 22	<i>I</i> ₄ 22
cell dimensions [<i>a</i> = <i>b</i> , <i>c</i> (Å)]	65.6, 178.6	68.1, 178.9	66.2, 179.9
resolution range (outer shell) (Å)	28.9–1.55 (1.65–1.55)	27.1–1.76 (1.87–1.76)	33.1–1.55 (1.63–1.55)
<i>R</i> _{sym} (%)	5.8 (108.2)	9.7 (100.6)	8.7 (38.8)
<i>I</i> /σ(<i>I</i>)	26.5 (2.94)	14.5 (2.28)	12.6 (2.10)
data completeness (%)	99.2 (99.4)	98.2 (91.5)	99.9 (100.0)
average redundancy	10.8 (10.4)	8.5 (7.4)	9.2 (4.0)
Wilson <i>B</i> factor (Å ²)	28.7	29.9	25.0
Refinement			
resolution (Å)	1.55	1.76	1.55
no. of reflections	27199	19932	28088
test set	1347	1059	1494
<i>R</i> (%)	17.6	18.9	23.3
<i>R</i> _{free} (%)	21.7	22.5	27.2
no. of protein atoms	1706	1568	1733
no. of other nonsolvent atoms	41	37	38
no. of solvent atoms	179	156	134
rmsd for bond lengths (Å)	0.020	0.019	0.017
rmsd for bond angles (deg)	2.051	1.844	1.609
average <i>B</i> factor (Å ²)	29.1	33.6	24.7

^aValues in parentheses pertain to outer resolution shell reflections. X-ray sources were located at the EMBL outstation at DESY.

deposited by the authors and protein-only model phases were used to calculate initial $2mF_o - DF_c$ and $mF_o - DF_c$ maps. On the basis of these maps, the structures were corrected as described in the main text and further refined against the original data. Corresponding refinement statistics are summarized in Table S1 of the Supporting Information. The revised versions of 1BJY and 1BJ0 have been deposited in the PDB as entries 4V2G and 4V2F, respectively.

RESULTS

TetR(D) was crystallized in the presence of 1 mM ATc and either 10 mM MgCl₂, 1 mM EDTA, or 2 M KCl. Isomorphous crystals that belonged to space group *I*₄22 and diffracted to 1.76 Å or better were obtained. The three structures were determined by molecular replacement as described in Experimental Procedures. Data collection and structure determination statistics are listed in Table 1.

In the presence of Mg²⁺ (Figure 2), the overall structure of TetR(D) bound to ATc is highly similar to that of the previously determined TetR(D)–[MgTc]⁺ complex (PDB entry 2TRT).^{3,4} The complete biological assemblies (i.e., the homodimers) of the two structures can be superposed with a *C*_α rmsd of 0.77 Å (396 superimposed atoms), as shown in Figure 2b. If only the ligand-binding domains (residues 48–208) are taken into account, a superposition of the dimers with a *C*_α rmsd of 0.52 Å (304 atoms) is obtained. In spite of the differences in chemical structure (Figure 1), the ATc and Tc molecules are positioned almost identically with respect to the binding pocket of TetR (Figure 3). The binding site itself as well as the conformations of the protein side chains lining it are also nearly identical. This means that the classical induced

conformation¹ is observed, with the C-terminal extremity of helix α6 unwound and residues 100–103 forming a type II β-turn instead. Compared to that in the Tc-containing structure, the positioning of the Mg²⁺ ion and its octahedral coordination sphere remain unchanged, with the metal liganding both oxygens of the ketoenolate moiety of ATc, the N_ε2 atom of the His100 side chain, and three water molecules (Figure 3b). The position and conformation of Thr103, which is hydrogen-bonded to one of the three water molecules via its hydroxyl group, are also unchanged. Thus, in the presence of Mg²⁺, the ATc-induced state of TetR(D) does not differ substantially from the known Tc-induced state.

The structure of the TetR(D)–ATc complex that was formed without Mg²⁺ in the presence of EDTA is shown in Figures 4 and 6. As anticipated, no electron density is observed at the position otherwise occupied by the Mg²⁺ ion (Figure 4a). Furthermore, none of the directly coordinated water ligands or any of the hydrogen-bonded water molecules that surround the Mg²⁺ ion in metal-containing structures^{1,5} are present. In fact, only a single ordered water molecule could be identified in the entire binding pocket. This molecule is doubly hydrogen-bonded to ATc from a position outside the plane of the ring system, at a distance of 3.0 Å from both keto–enol oxygens. Presumably, the remaining space around ATc is filled with disordered water molecules, which are not visible in the electron density because of their dynamic nature.

Despite the absence of the metal and its stably associated water molecules, TetR(D) is found to adopt a fully induced conformation (Figures 4b and 6). Moreover, the dimer structure is essentially indistinguishable from that of the complex with [MgATc]⁺ (*C*_α rmsd of 0.40 Å for 404 superimposed atoms) and the previously determined structure

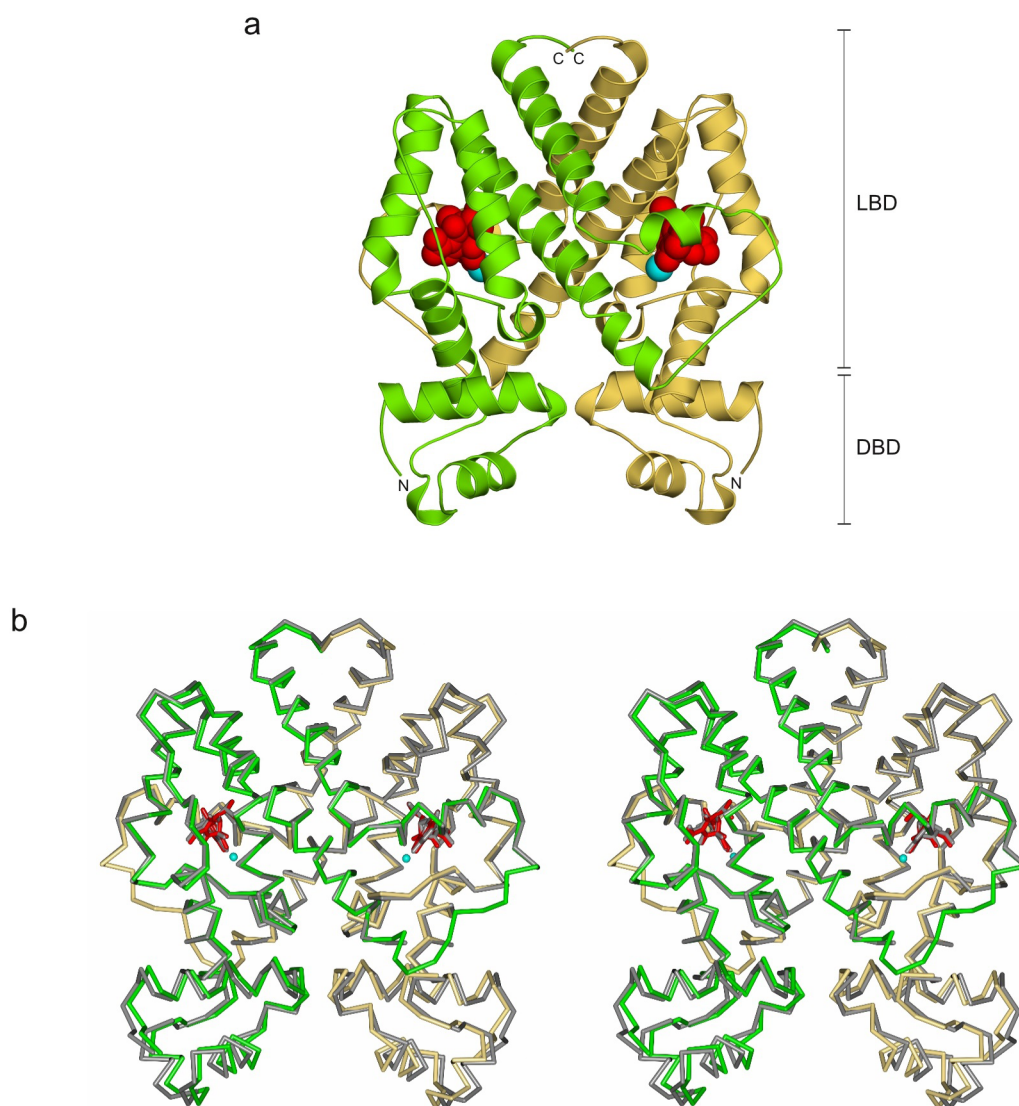


Figure 2. Structure of TetR(D) in complex with $[\text{MgATc}]^+$. (a) Ribbon diagram of the overall dimer structure, with TetR(D) monomers colored green and yellow. The ligand-binding domain (LBD) and DNA-binding domain (DBD) have been indicated. The bound ATc molecules and Mg^{2+} ions are shown in space-filling representation (red and cyan, respectively). (b) Stereoview showing a comparison to the previously determined structure of TetR(D) in complex with $[\text{MgTc}]^+$ (PDB entry 2TRT). Proteins are represented as C_α traces, and the superposed $[\text{MgTc}]^+$ complex is colored gray. Antibiotic molecules are depicted as stick models with spheres representing Mg^{2+} .

of the TetR(D)– $[\text{MgTc}]^+$ complex (PDB entry 2TRT, C_α rmsd of 0.62 Å for 396 superimposed atoms). Values for the ligand-binding domains alone are 0.42 Å (312 atoms) and 0.39 Å (304 atoms), respectively. Strikingly, the His100 and Thr103 side chains, which would otherwise interact with the metal or the water molecules in its coordination sphere, occupy the exact same positions as in the Mg^{2+} -containing complex. In the absence of Mg^{2+} , the side chain of His100 forms a direct hydrogen bond with the keto–enol moiety of ATc, whereas Thr103 continues to stabilize the conformation of the β -turn via the usual hydrogen bond of its side chain to the main chain carbonyl of His100. Another residue that helps to maintain the induced conformation in a metal-independent way is Pro105, which engages in a hydrophobic interaction with the ATc ring system. In addition, the solitary water molecule in the binding site, which is hydrogen-bonded to the ketoenolate moiety of ATc, is also within 3.5 Å of the backbone nitrogen of Pro105 and the carbonyl oxygen of Thr103 and may therefore

contribute to stabilization of the region via an additional hydrogen bond.

The complex that was crystallized without Mg^{2+} in the presence of 2 M KCl is shown in Figures 5 and 6. Unlike Mg^{2+} , K^+ did not enhance the binding of ATc to TetR(D) in fluorescence-monitored binding assays, its addition resulting in an association constant ($K_a = 2.3 \times 10^7 \text{ M}^{-1}$) very similar to that which we observed in the presence of equivalent amounts of Na^+ ($K_a = 2.5 \times 10^7 \text{ M}^{-1}$). Apparently, monovalent ions interact only weakly with the complex and do not stabilize it to the extent that divalent metal ions do. Because of the elevated KCl concentration in our crystallization assay, a K^+ ion is nevertheless present in the structure. Giving rise to local electron density much stronger than that of a typical water molecule or Na^+ , the K^+ ion is readily identified in the $2mF_o - DF_c$ map (Figure 5a). Interestingly, its position is markedly different from that of Mg^{2+} in the TetR(D)– $[\text{MgATc}]^+$ complex (Figure 5b). Rather than replacing Mg^{2+} , the monovalent ion takes the position of one of the water ligands,

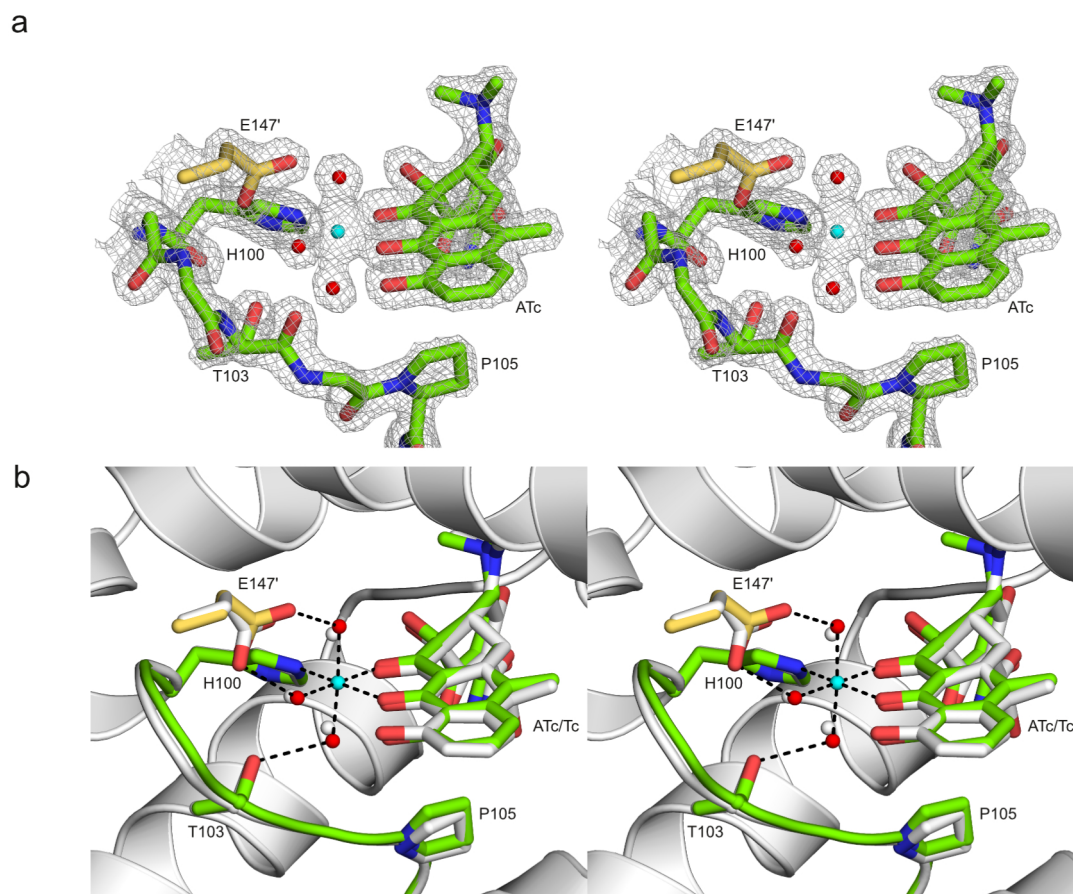


Figure 3. Detailed view of the ligand-binding site of TetR(D) in complex with [MgATc]⁺. The Mg²⁺ ion is colored cyan. (a) Stereoview showing the electron density map ($2mF_o - DF_c$ contoured at 1.5σ) for the Mg²⁺-proximal section of the ligand-binding pocket, together with the final model. (b) Stereoview of the ligand-binding pocket with the superposed TetR(D)-[MgTc]⁺ complex colored gray. In the structure with [MgATc]⁺, Mg²⁺ coordination and hydrogen bonds are represented by black dotted lines.

outside of the plane of the ATc ring system, whereas the original Mg²⁺ position remains unoccupied. This arrangement, presumably a consequence of the larger radius of the K⁺ ion, is reminiscent of an earlier crystal structure of oxytetracycline, in which K⁺ is similarly bound to the antibiotic in an out-of-plane position.²³ In spite of the unusual placement of the ion and the surrounding water molecules, which has not been observed in any previously determined TetR structure, the repressor itself remains fully induced. Its structure is very similar to that of the complex with Mg²⁺ (C_α rmsd of 0.86 Å for 388 superimposed atoms), that of the complex without metal ions (C_α rmsd of 0.74 Å for 388 atoms), and that of the complex with [MgTc]⁺ (PDB entry 2TRT, C_α rmsd of 0.44 Å for 390 atoms). Values for ligand-binding domains alone are 0.45 Å (296 atoms), 0.33 Å (296 atoms), and 0.34 Å (298 atoms), respectively. Like in the metal-free structure, the His100 and Thr103 side chains are kept in place by Mg²⁺-independent hydrogen bonds to the antibiotic and the protein backbone, respectively (Figure 5b).

The structures presented here argue against a distinct induction mode specific for ATc as well as against the dependence of the standard induction mechanism on the presence of Mg²⁺. This result is rather unexpected, particularly because in an earlier report Orth et al.⁸ had claimed that divalent metal ions are essential for induction of TetR by CTc. We therefore reanalyzed the data and models from this earlier study. PDB entry 1BJY corresponds to the structure that resulted from cocrystallization of TetR with CTc in the absence

of Mg²⁺, termed form “[3]” in the original report.⁸ Figure 7a shows a difference map ($mF_o - DF_c$) for PDB entry 1BJY, calculated using the experimental structure factors as deposited by the authors and protein-only model phases. The metal-free ligand of the deposited model shows a poor fit to the electron density, the twisted shape of which strongly suggests that degradation of CTc to iso-CTc¹³ has occurred. Unlike most other tetracyclines, CTc readily undergoes isomerization even at neutral pH, particularly in the absence of divalent metal ions.¹³ Moreover, Orth et al. note that their cocrystallization assay involved incubation at room temperature for up to 2 weeks.⁸ On the basis of these considerations, we revised the original model and replaced CTc with iso-CTc. As a result, the R factor for this structure decreased from 20.3 to 17.5% and R_{free} from 26.5 to 25.2% (Table S1 of the Supporting Information).

The second Mg²⁺-free structure reported by Orth et al., 1BJ0 (or form “[2]” in the original report), was also reanalyzed. Figure 7b shows the corresponding $2mF_o - DF_c$ and $mF_o - DF_c$ maps, calculated using protein-only model phases. Here, the complete lack of density for CTc suggests that the ligand was no longer bound at all, presumably as a consequence of the major decrease in affinity that accompanies the loss of Mg²⁺.⁹ Therefore, we corrected this model by refining it without the ligand. In this case, our revision decreased R from 24.2 to 20.8% and R_{free} from 32.4 to 27.8% (Table S1 of the Supporting Information).

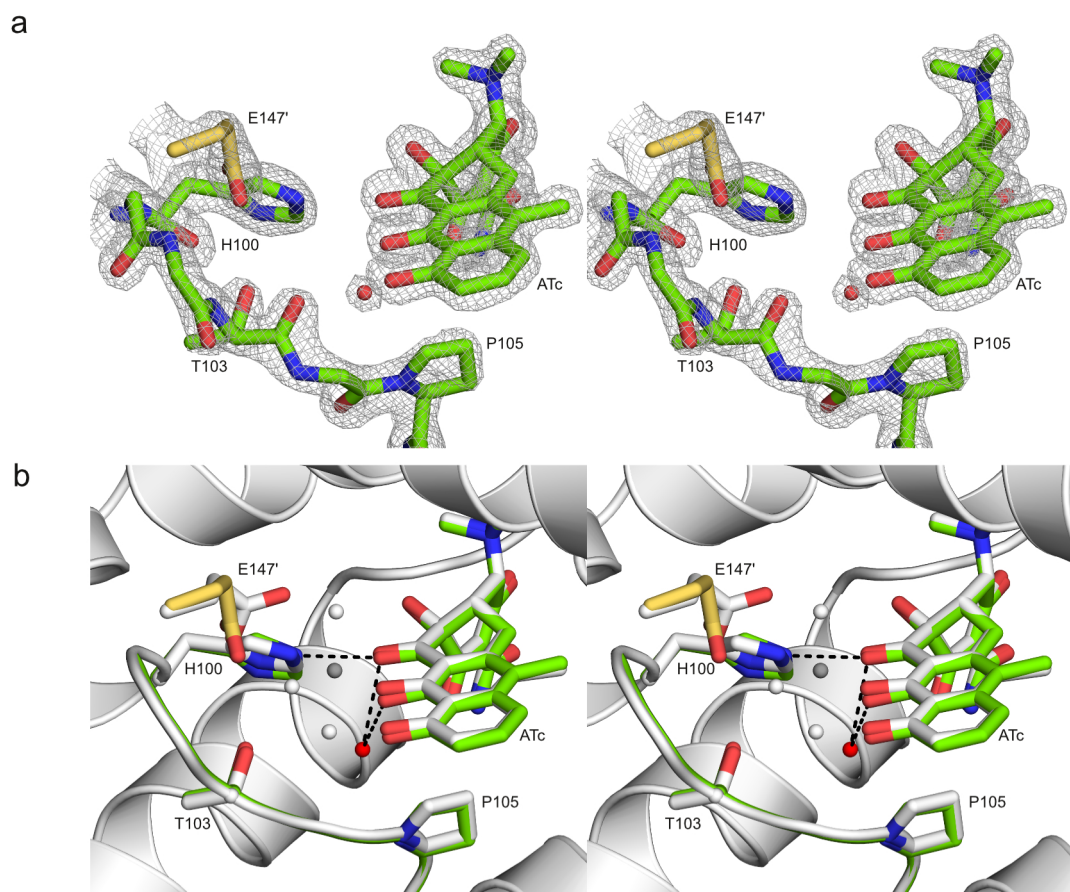


Figure 4. Structure of TetR(D) in complex with ATc, crystallized without Mg^{2+} in the presence of EDTA. (a) Stereoview showing the electron density map ($2mF_o - DF_o$, contoured at 1.5σ) for the Mg^{2+} -interacting region, together with the final model. (b) Stereoview of the ligand-binding pocket with the superposed model of the TetR(D)-[MgATc] $^{+}$ complex colored gray. Hydrogen bonds in the metal-free complex are shown as black dotted lines.

DISCUSSION

Tetracyclines are strong chelators of divalent metal ions and *in vivo* predominantly exist in complex with Mg^{2+} .¹⁰ The presence of this ion contributes to the affinity of TetR for the antibiotic, typically resulting in association constants (K_a) that are 3–4 orders of magnitude higher and reach levels of $\geq 10^9 \text{ M}^{-1}$.¹ Physiologically, these high affinity constants are important to ensure that antibiotic resistance is fully activated before ribosome binding ($K_a \approx 10^6 \text{ M}^{-1}$) and resulting toxicity set in.

Detailed mechanisms that have been proposed for TetR induction by tetracyclines comprise a sequence of separate events,^{1,5,8,11} starting with rigid binding of the antibiotic to a structurally invariant part of the binding pocket. Initial binding is thought to precisely position the associated Mg^{2+} ion, which is subsequently recognized by conserved residues His100 and Thr103. In moving toward the ion, these residues would then drive early conformational changes, in particular unwinding of the C-terminal extremity of helix $\alpha 6$ and formation of a type II β -turn by residues 100–103. These changes, in turn, lead to further downstream events and, ultimately, a rotational motion of helix $\alpha 4$ and a concomitant pendulum-like displacement of the DNA-binding domains of the protein dimer. Thus, the allosteric models are characterized by stepwise structural changes and a strict dependence on Mg^{2+} recognition by key residues.

Paradoxically, the observation that the Tc derivative ATc is able to release TetR from promoters in the absence of divalent

metal ions⁹ appears to contradict models that hinge on Mg^{2+} recognition. To reconcile their ATc data with the existing theory, Scholz et al. proposed that induction by the Mg^{2+} -free antibiotic might occur via a structurally unrelated, presently uncharacterized interaction mode.⁹ Given the unique chemical structure of ATc (Figure 1), which not only lacks a hydroxyl substituent but also features an extended aromatic system, such a Mg^{2+} -independent mechanism could be specific for this particular derivative. This would explain why induction in the absence of Mg^{2+} has not been observed with Tc or other derivatives.¹¹

The crystallographic results presented here do not lend support to the hypothesis of an alternative allosteric mechanism for ATc but, on the contrary, suggest that induction by this derivative does not differ substantially from the extensively characterized induction mode of unmodified Tc (7H-Tc) and other tetracyclines. Moreover, the canonical induced state is observed in the presence and absence of Mg^{2+} . A further complex that we analyzed, containing K^{+} instead of Mg^{2+} , shows the same protein conformation despite an out-of-plane positioning of the monovalent ion and the presence of a novel hydration pattern around the ion and ATc. This pattern differs considerably from that observed in previous high-resolution structures of TetR–antibiotic complexes. The intricate metal-dependent network of water molecules among tetracyclines, Mg^{2+} , and TetR, sometimes termed a “water zipper”, has been discussed extensively in earlier literature and was thought to

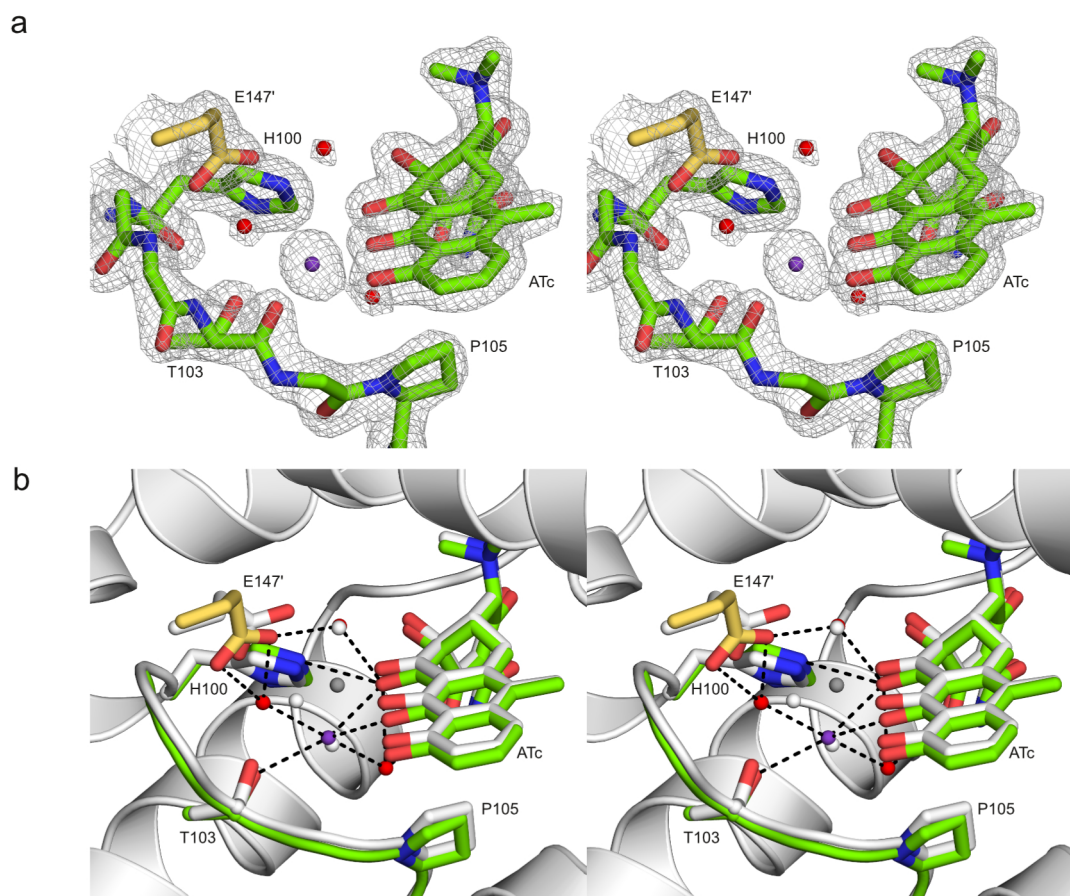


Figure 5. Structure of TetR(D) in complex with ATc, crystallized without Mg^{2+} in the presence of 2 M KCl. The K^+ ion is colored purple. (a) Stereoview showing the electron density map ($2mF_o - DF_o$, contoured at 1.2σ) for the metal-interacting site, together with the final model. (b) Stereoview of the ligand-binding pocket with the superposed model of the TetR(D)-[MgATc] $^+$ complex colored gray. Hydrogen bonds in the K^+ -containing complex are shown as black dotted lines.

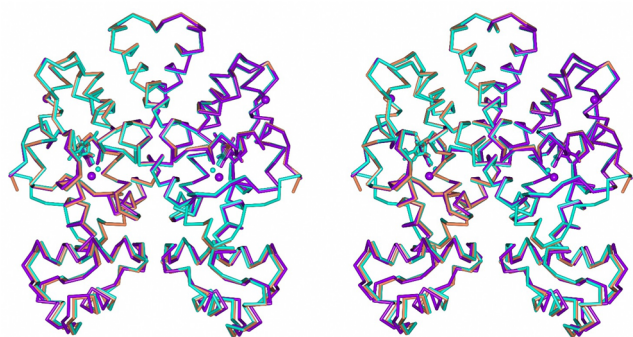


Figure 6. Superposition of all three structures of TetR(D) with ATc that were determined in this study. Cyan for the complex with [MgATc] $^+$, brown for the complex without Mg^{2+} in the presence of EDTA, and purple for the complex without Mg^{2+} in the presence of K^+ .

play a major role in the allosteric mechanism.^{1,5} However, the structures presented here show that induction still takes place if this network is either drastically altered, as in our structure with K^+ , or entirely absent, as in the structure without ions.

Taken together, our data suggest that the known induced state of the repressor is considerably more robust than anticipated and largely insensitive to changes in both metal association and hydration pattern. Once the ligand is bound, Mg^{2+} -independent contacts between TetR and the antibiotic

molecule apparently suffice to lock the region between amino acids His100 and Thr103 in its induced conformation, which is linked to downstream allosteric effects as observed in molecular dynamics simulations by Aleksandrov et al.¹¹ Mg^{2+} -independent interactions that are relevant in this respect include the hydrophobic contact between Pro105 and the ring system, as well as the now direct (rather than Mg^{2+} -mediated) interaction of His100 with the keto-enol moiety of the antibiotic. Interestingly, none of these contacts are specific for ATc, suggesting that induction should also occur with Tc or other derivatives if these compounds were bound in the absence of Mg^{2+} .

Our unexpected observations prompted us to review the available evidence for metal-triggered repressor allostery. Although several highly detailed induction models have been proposed in earlier work,^{1,8,11} these studies invariably assume a strict metal dependence and refer back to a single crystallographic study by Orth et al.⁸ As we have shown here, this study of metal-free TetR(D)-CTc complexes contains major technical flaws that invalidate its conclusions. In our revised models, the metal-free structures either completely lack CTc or contain the degradation product iso-CTc. Because of its interrupted planarity and freely rotating bond between two pairs of rings, iso-CTc behaves in a manner very different from that of actual tetracyclines and is known to bind TetR in an aberrant, noninducing manner.¹³ Iso-CTc is therefore by no means representative of Mg^{2+} -free tetracyclines, and its binding

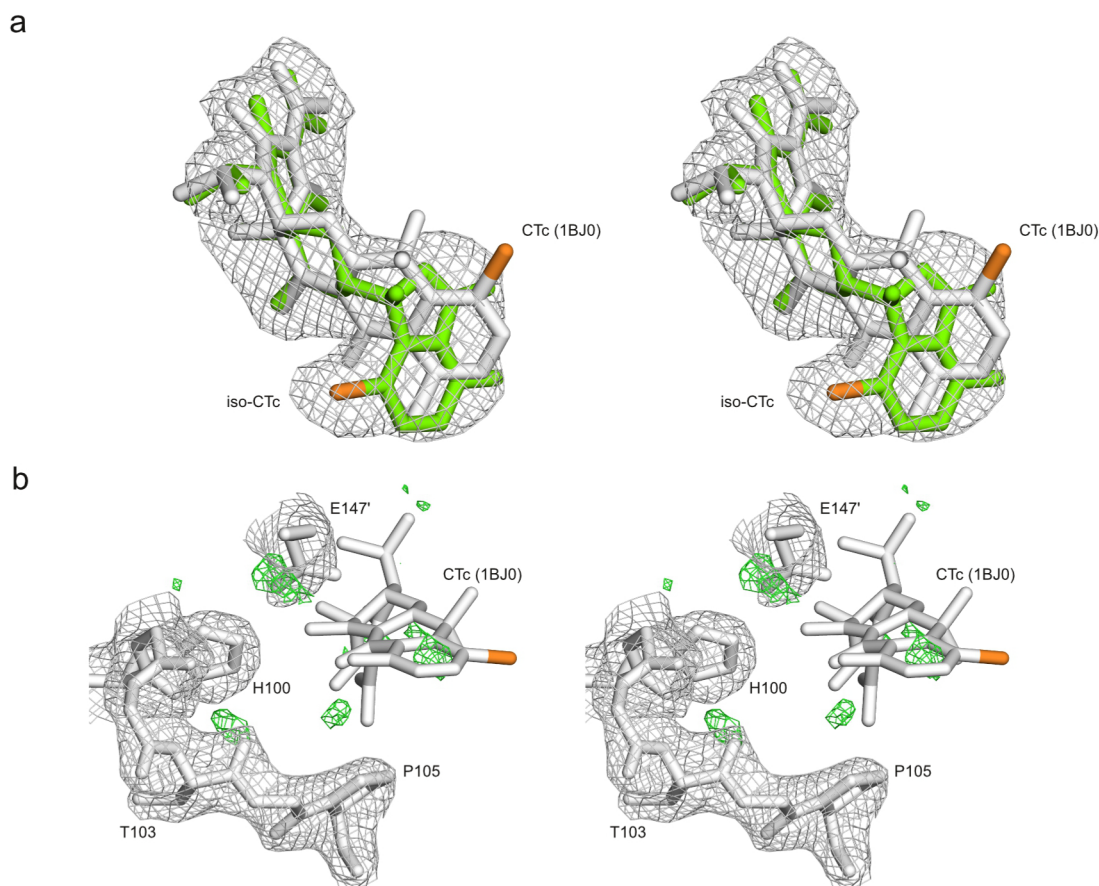


Figure 7. Revision of the earlier crystal structures of PDB entries 1BJY and 1BJ0 by Orth et al.⁸ These two crystal structures, in which a single binding site (1BJY) or both binding sites (1BJ0) of the TetR homodimer contain Mg^{2+} -free CTc and nevertheless retain the uninduced conformation, were considered direct evidence of a metal-triggered allosteric mechanism.⁸ (a) Comparison of the CTc molecule in the noninduced binding site of 1BJY (gray) and our corrected model containing iso-CTc (green). Also shown is an $mF_o - DF_c$ map, calculated using protein-only model phases, contoured at 2.5σ . The Cl atom, which is expected to give rise to strong local electron density, is colored orange in both models. (b) Revision of 1BJ0. Shown are $2mF_o - DF_c$ (1.0σ , gray) and $mF_o - DF_c$ (2.5σ , green) density maps of the binding site, calculated using protein-only model phases. Clearly, the presence of the CTc ligand in 1BJ0 (gray stick model, with Cl colored orange) is not supported by these maps.

mode merely illustrates the importance of a rigid, approximately coplanar ring system for TetR induction.

In summary, our results clearly argue against a markedly different ATc-specific induction mode and distinct Mg^{2+} -dependent and -independent pathways, concepts that had been proposed in earlier work.^{9,11} Rather, our data point at a universal mechanism for all inducers, which does not strictly require Mg^{2+} as long as the antibiotic is still efficiently bound by the repressor in the absence of the metal. Of all currently described Tc derivatives, ATc possesses the highest affinity for TetR, with a K_a of $9.8 \times 10^{11} M^{-1}$ in the presence and $6.5 \times 10^7 M^{-1}$ in the absence of Mg^{2+} .⁹ These association constants are 500-fold higher than for Tc, allowing repressor saturation by ATc even in the absence of divalent metal ions, under experimental conditions where the affinity of Tc and other derivatives would be insufficient for quantitative binding and derepression. Although the presence of a Mg^{2+} ion clearly leads to additional stabilization of the induced state, we conclude that there is no evidence of the purely metal-triggered allostery that was postulated in earlier reports.

■ ASSOCIATED CONTENT

⑤ Supporting Information

Refinement statistics for the revised structures 4V2F and 4V2G (Table S1). This material is available free of charge via the Internet at <http://pubs.acs.org>.

■ AUTHOR INFORMATION

Corresponding Authors

*E-mail: sebastiaan.werten@uni-greifswald.de. Phone: +49 38 34 86 44 61. Fax: +49 38 34 86 43 73.

*E-mail: winfried.hinrichs@uni-greifswald.de.

Author Contributions

S.W. and D.D. contributed equally to this work.

Notes

The authors declare no competing financial interest.

■ ACKNOWLEDGMENTS

Britta Girbardt and Leona Berndt are gratefully acknowledged for technical assistance. We also thank the beamline staff at the EMBL at DESY for assistance during crystallographic data collection, as well as Fabrice Klein for critical reading of the manuscript.

■ ABBREVIATIONS

TetR, tetracycline repressor; TetR(D), tetracycline repressor (class D); Tc, tetracycline; ATc, 5a,6-anhydrotetracycline; CTC, 7-chlorotetracycline; iso-CTC, 6-iso-7-chlorotetracycline; EDTA, ethylenediaminetetraacetic acid; rmsd, root-mean-square deviation.

■ REFERENCES

- (1) Saenger, W., Orth, P., Kisker, C., Hillen, W., and Hinrichs, W. (2000) The Tetracycline Repressor: A Paradigm for a Biological Switch. *Angew. Chem., Int. Ed.* 39, 2042–2052.
- (2) Cuthbertson, L., and Nodwell, J. R. (2013) The TetR Family of Regulators. *Microbiol. Mol. Biol. Rev.* 77, 440–475.
- (3) Hinrichs, W., Kisker, C., Düvel, M., Müller, A., Tovar, K., Hillen, W., and Saenger, W. (1994) Structure of the Tet Repressor-Tetracycline Complex and Regulation of Antibiotic Resistance. *Science* 264, 418–420.
- (4) Kisker, C., Hinrichs, W., Tovar, K., Hillen, W., and Saenger, W. (1995) The Complex Formed between Tet Repressor and Tetracycline-Mg²⁺ Reveals Mechanism of Antibiotic Resistance. *J. Mol. Biol.* 247, 260–280.
- (5) Orth, P., Cordes, F., Schnappinger, D., Hillen, W., Saenger, W., and Hinrichs, W. (1998) Conformational Changes of the Tet Repressor Induced by Tetracycline Trapping. *J. Mol. Biol.* 279, 439–447.
- (6) Orth, P., Schnappinger, D., Hillen, W., Saenger, W., and Hinrichs, W. (2000) Structural Basis of Gene Regulation by the Tetracycline Inducible Tet Repressor-Operator System. *Nat. Struct. Biol.* 7, 215–219.
- (7) Reichheld, S. E., Yu, Z., and Davidson, A. R. (2009) The Induction of Folding Cooperativity by Ligand Binding Drives the Allosteric Response of Tetracycline Repressor. *Proc. Natl. Acad. Sci. U.S.A.* 106, 22263–22268.
- (8) Orth, P., Saenger, W., and Hinrichs, W. (1999) Tetracycline-Chelated Mg²⁺ Ion Initiates Helix Unwinding in Tet Repressor Induction. *Biochemistry* 38, 191–198.
- (9) Scholz, O., Schubert, P., Kintrop, M., and Hillen, W. (2000) Tet Repressor Induction without Mg²⁺. *Biochemistry* 39, 10914–10920.
- (10) Palm, G. J., Lederer, T., Orth, P., Saenger, W., Takahashi, M., Hillen, W., and Hinrichs, W. (2008) Specific Binding of Divalent Metal Ions to Tetracycline and to the Tet Repressor/Tetracycline Complex. *J. Biol. Inorg. Chem.* 13, 1097–1110.
- (11) Aleksandrov, A., Schuldt, L., Hinrichs, W., and Simonson, T. (2008) Tet Repressor Induction by Tetracycline: A Molecular Dynamics, Continuum Electrostatics, and Crystallographic Study. *J. Mol. Biol.* 378, 898–912.
- (12) Ettner, N., Müller, G., Berens, C., Backes, H., Schnappinger, D., Schreppe, T., Pfeleiderer, K., and Hillen, W. (1996) Fast Large-Scale Purification of Tetracycline Repressor Variants from Overproducing *Escherichia coli* Strains. *J. Chromatogr., A* 742, 95–105.
- (13) Volkers, G., Petruschka, L., and Hinrichs, W. (2011) Recognition of Drug Degradation Products by Target Proteins: Isotetracycline Binding to Tet Repressor. *J. Med. Chem.* 54, 5108–5115.
- (14) Otwinowski, Z. (1993) Data Collection and Processing. *Proceedings of the CCP4 Study Weekend 1993*, pp 55–62, Daresbury Laboratory, Warrington, U.K.
- (15) Kabsch, W. (2010) XDS. *Acta Crystallogr. D* 66, 125–132.
- (16) Collaborative Computational Project, Number 4 (1994) The CCP4 Suite: Programs for Protein Crystallography. *Acta Crystallogr. D* 50, 760–763.
- (17) Navaza, J. (2001) Implementation of Molecular Replacement in AMoRe. *Acta Crystallogr. D* 57, 1367–1372.
- (18) Emsley, P., and Cowtan, K. (2004) Coot: Model-Building Tools for Molecular Graphics. *Acta Crystallogr. D* 60, 2126–2132.
- (19) Emsley, P., Lohkamp, B., Scott, W. G., and Cowtan, K. (2010) Features and Development of Coot. *Acta Crystallogr. D* 66, 486–501.

- (20) Murshudov, G. N., Vagin, A. A., and Dodson, E. J. (1997) Refinement of Macromolecular Structures by the Maximum-Likelihood Method. *Acta Crystallogr. D* 53, 240–255.
- (21) Murshudov, G. N., Skubák, P., Lebedev, A. A., Pannu, N. S., Steiner, R. A., Nicholls, R. A., Winn, M. D., Long, F., and Vagin, A. A. (2011) REFMAC5 for the Refinement of Macromolecular Crystal Structures. *Acta Crystallogr. D* 67, 355–367.
- (22) McNicholas, S., Potterton, E., Wilson, K. S., and Noble, M. E. M. (2011) Presenting Your Structures: The CCP4mg Molecular-Graphics Software. *Acta Crystallogr. D* 67, 386–394.
- (23) Jogun, K. H., and Stezowski, J. J. (1976) Chemical-Structural Properties of Tetracycline Derivatives. 2. Coordination and Conformational Aspects of Oxytetracycline Metal Ion Complexation. *J. Am. Chem. Soc.* 98, 6018–6026.